Journal of Inorganic and General Chemistry
ZAAC
Zeitschrift für anorganische und allgemeine Chemie
DOI: 10.1002/zaac.202000034
ARTICLE

Small Chains of Main Group Elements by BH_3 Adduct Formation of tBu_2E-N(H)-$EtBu_2$ (E = P, As)

Maximilian Fritz,[a] Leon Maser,[b] Benjamin Ringler,[a] Carsten von Hänisch,[a] and Robert Langer*[a,b]

Dedicated to Prof. Manfred Scheer on the Occasion of his 65th Birthday

Abstract. Borane adducts of *bis*(di-*tert*-butylphosphanyl)amine (**1a**) and *bis*(di-*tert*-butylarsino)amine (**1b**) are reported. Based on quantum-chemical investigations in combination with experimental results, it is demonstrated that the tautomerism known for tBu_2P-N(H)-$PtBu_2$ (**1a**), can be observed for the mono adduct tBu_2P-N(H)-$P(BH_3)tBu_2$ (**2a**) as well, whereas for the corresponding arsenic compound **2b** only one stable isomer is found. The *bis*-borane adduct $tBu_2(BH_3)As$-N(H)-$As(BH_3)tBu_2$ (**3b**) is a rare example of a structurally characterized, tertiary arsine borane adduct, which can be directly compared with the corresponding phosphorus compound $tBu_2(BH_3)P$-N(H)-$P(BH_3)tBu_2$ (**3a**). Deprotonation of mixtures containing **2a** by *n*BuLi leads to the lithium-containing coordination polymer **4a**, in which the actual chain consists only of non-carbon atoms.

Introduction

The utilization of BH_3 groups for the protection of all kind of phosphines is a common strategy to prevent oxidation of phosphorus(III) compounds under aerobic conditions.[1–4] These phosphine boranes can be used as bench-stable pre-ligands or to facilitate substitution at the phosphorus, which can even lead to the introduction of chirality at the phosphorus atom.[5] In connection with a suitable transition metal fragment, the reactivity of such phosphine boranes can result in novel boron-containing species.[6–8] In this context, we recently discovered the re-arrangement of an iron phosphine borane to a novel type of boron-based pincer complex and became therefore interested in BH_3 adducts of diphosphines with a small bite angle such as *bis*(diphenylphosphanyl)amine [dppa = Ph_2P-N(H)-PPh_2]. Depending on the substituents at the phosphorus center, very different reactivities can be observed in combination with metal precursors. As *tert*-butyl substituents usually increase the stability of the complexes and prevent intramolecular C-H-activation, tBu_2P-N(H)-$PtBu_2$ (**1a**) and its conceivable borane adducts came into the focus of our interest.[9] An interesting feature of this class of compounds is that, for certain substituents an equilibrium with a tautomer (**1a^1**) is observed.[9]

For the heavier homologue arsenic, a number of arsines including tBu_2As-N(H)-$AstBu_2$ are well-known,[10] but their corresponding BH_3 adducts[11–13] as well as adducts with haloboranes are in contrast exceedingly rare.[14,15]

Oligomers and polymers, in which the main chain is based on elements other than carbon, gained increasing attention in recent years.[16–34] Recent efforts to develop novel oligo- and polymers based on group 13 and 15 elements resulted in the stepwise construction of small chains of pnictogenyl boranes,[35–39] some of them stabilized in the coordination sphere of a transition metal.[11,35,40–42] In analogy to oligomeric phosphanyl- and arsanyl-boranes, **1a** and its deprotonated analogue can potentially serve as building blocks for new polymeric materials based on main group elements. With the aim to prepare simple chains containing group 13 and 15 elements, we targeted borane adducts of tBu_2E-N(H)-$EtBu_2$ (**1**, E = P, As) as promising candidates. In the present manuscript, we report our results on the reactivity of **1** towards BH_3·THF and compare the relative stability of the reaction products and their isomers.

Results and Discussion

The equilibrium in solution between *bis*(di-*tert*-butylphosphanyl)-amine (**1a**) and its tautomer **1a^1** (Scheme 1) indicates that the phosphorus and nitrogen atoms in such compounds are in principle capable of binding Brønsted or Lewis acids. With one lone pair mainly located at the nitrogen atom and two lone pairs located at the phosphorus atoms, these types of molecules exhibit three potential binding sites for BH_3 groups.

Addition of one equivalent of BH_3·THF to solutions of **1a**/**1a^1** leads to a mixture of compounds in the $^{31}P\{^1H\}$ NMR spectrum (Figure 1). A comparison with the corresponding ^1H-coupled ^{31}P NMR spectrum revealed the presence of different

* Prof. Dr. R. Langer
E-Mail: robert.langer@chemie.uni-halle.de
[a] Department Chemistry
Philipps-Universität Marburg
Hans-Meerwein-Str.
35032 Marburg, Germany
[b] Institute of Chemistry, Natural Science Faculty II
Martin-Luther-Universität Halle-Wittenberg
Kurt-Mothes-Str. 2
06120 Halle/S., Germany
Supporting information for this article is available on the WWW under **http://dx.doi.org/10.1002/zaac.202000034** or from the author.

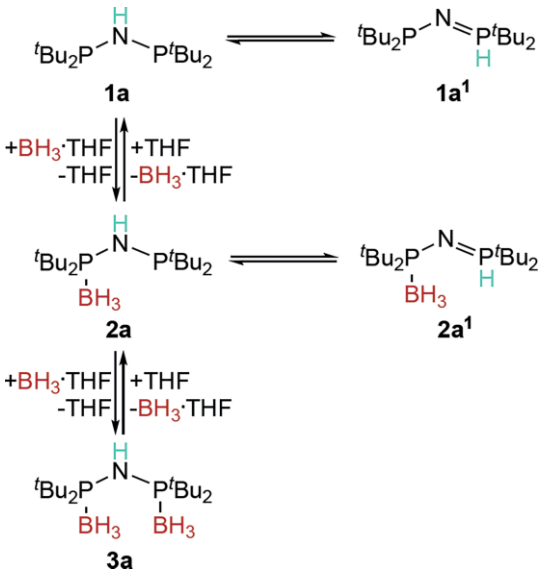

Scheme 1. Reactivity of **1a** and its tautomer **1a¹** in the presence of different amounts of BH_3·THF.

tautomers containing a phosphorus bound hydrogen atom. In addition to the starting material **1a** and its tautomer **1a¹**, we observed the mono adduct **2a¹** that gives rise to a doublet resonance at δ = 38.9 ppm ($^2J_{PP}$ = 14.5 Hz) and a broad resonance at δ = 94.3 ppm. The corresponding tautomer **2a** displays a doublet resonance at δ = 76.0 ppm ($^2J_{PP}$ = 32.7 Hz) and a multiplet at δ = 78.6 ppm in the $^{31}P\{^1H\}$ NMR spectrum of the reaction mixture. Despite the fact we used exactly one equivalent of BH_3·THF, we observed the *bis*-borane adduct **3a** in the mixture with **1a**, **2a** and their respective tautomers (Scheme 1). However, the utilization of less than two equivalents of BH_3·THF in these reactions always leads to mixtures, for which all attempts to isolate a pure compound remained unsuccessful, so far. Furthermore, performing the reaction at low temperatures or in lower concentrations did not affect the selectivity significantly.

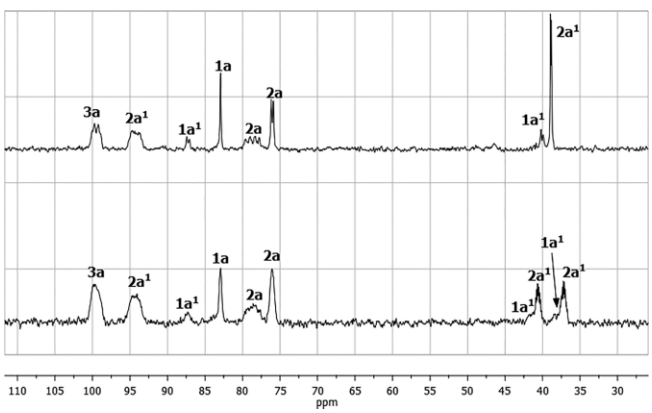

Figure 1. $^{31}P\{^1H\}$ NMR spectrum of the reaction of **1a** with one equivalent BH_3·THF (top). The corresponding ^{31}P NMR spectrum is shown in the bottom.

Interestingly, the reaction of **1a/1a¹** with two equivalents of BH_3·THF results in the clean formation of a single compound according to the $^{31}P\{^1H\}$ NMR spectrum (δ_P = 99.5 ppm), which was identified as the borane adduct **3a** with two BH_3 groups attached to the two phosphino groups (Scheme 2). The $^{11}B\{^1H\}$ NMR spectrum of **3a** exhibits a doublet resonance at –37.9 ppm ($^1J_{BP}$ = 78.1 Hz), but the resonances of the boron-bound hydrogen atoms are absent in the ^1H NMR spectrum and can be observed as doublet of doublet resonances at δ = 1.47 ppm ($^2J_{HP}$ = 12.8, $^4J_{HH}$ = 3.7 Hz) upon ^{11}B-decoupling of the ^1H NMR spectrum. An analysis of IR spectra supported the formation of **3a** with three diagnostic bands at 2442, 2384, and 2347 cm^{-1} assignable to B–H stretching vibrations.

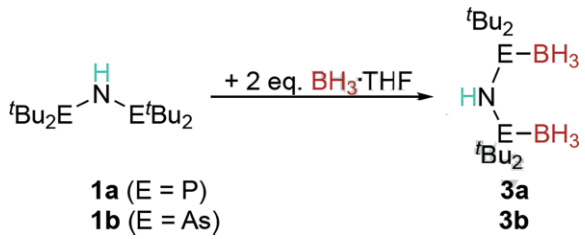

Scheme 2. Reaction of **1** with two equivalents of BH_3·THF.

The identity of **3a** was finally confirmed by single crystal X-ray diffraction. The molecular structure of **3a** in the solid state (Figure 2) displays a *bis*-borane adduct of **1a** with a BH_3 group bound to each phosphorus atom. These findings clearly indicate that the nitrogen atom in **1a** does not readily bind BH_3, which is in agreement with the spectroscopic data in solution, where only one resonance for the *bis* adduct **3a** was observed. Compared to the corresponding phenyl-substituted derivative, $Ph_2P(BH_3)$-NH-$P(BH_3)Ph_2$,[43] slightly longer P–N and P–B distances as well as larger P–N–P angles are observed for **3a**. These findings are likely a result of the increased bulk of *tert*-butyl groups and the less favored π-delocalization of the nitrogen-based lone pair.

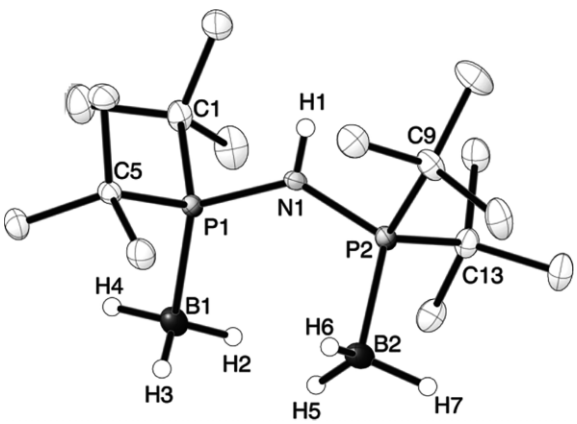

Figure 2. Molecular structure of **3a** in the solid state (carbon-bound hydrogen atoms are omitted for clarity, thermal ellipsoids are set at 50 % probability).

A similar result is observed in the reaction of the corresponding arsenic compound **1b** with two equivalents

BH_3·THF, which results in the formation of the *bis*-borane adduct **3b**. The analogous reaction with one equivalent leads to mixtures of compounds, but all attempts to exactly identify the reaction products remained unsuccessful.

In a similar manner to **3a**, compound **3b** gives rise to a broad resonance at –37.6 ppm in the $^{11}B\{^1H\}$ NMR spectrum, whereas the resonances of boron-bound hydrogen atoms are absent in the ^1H NMR spectrum and only observable upon ^{11}B-decoupling at δ = 1.66 ppm. The IR spectrum exhibits three bands at 2440, 2406 and 2356 cm^{-1} for the B–H stretching vibration. Single crystal X-ray diffraction experiments revealed a molecular structure of **3b** in solid state (Figure 3) similar to **3a**. Table 1 summarizes and compares selected bond lengths and angles.

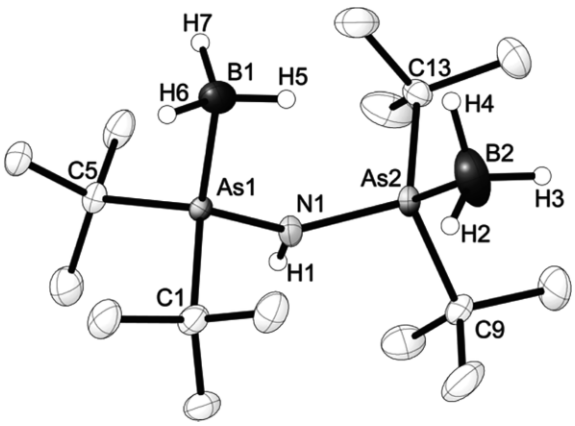

Figure 3. Molecular structure of **3b** in the solid state (carbon-bound hydrogen atoms are omitted for clarity, thermal ellipsoids are set at 50% probability).

Table 1. Selected distances and angles of **3a** and **3b** in the solid state.

Bond /Å, angle /°	E = P	E = As
E–N	1.706(1)–1.710(1)	1.829(2)–1.834(2)
E–B	1.921(2)–1.931(2)	2.037(3)–2.038(3)
E–C	1.869(1)–1.877(2)	1.983(2)–1.993(2)
E–N–E	136.8(1)	132.3(1)
B–E···E–B	43.1(1)	45.2(1)

In accordance with the increased value of the covalent radius of arsenic relative to phosphorus, the As–N, As–B, and As–C distances in **3b** are significantly longer (> 0.1 Å) than the P–N, P–B, and P–C distances in **3a**, respectively (Table 1). The E–N–E angle in **3a** (E = P) is with 136.8° slightly larger than in **3b** with 132.3° (E = As). The dihedral angle between the planes formed by one boron and two pnictogen atoms E (E = P, As), respectively, is only slightly different in **3a** (43.1°) and **3b** (45.2°).

Due to the fact that no mono adduct such as **2a** is selectively formed in the reaction with one equivalent of BH_3·THF and the observation that the BH_3 group preferable binds to phosphorus or the arsenic atom, we started to investigate this system by quantum-chemical methods. Using density functional theory (B97D/def2-TZVPP), we compared the relative Gibbs energy of the optimized structures of different isomers of **2** and **3**. Considering different positions for BH_3-binding, we compared the relative Gibbs energy $\Delta G°$(298 K) of the optimized geometries for **2a**, **2b** and the different isomers **2a$^{1–3}$** and **2b$^{1–3}$** (Table 2 and Table 3). For E = P the two isomers **2a** and **2a^1** were calculated to be the most stable ones and exhibit very similar energies. In this case, **2a^1** was calculated to be more stable by 15.1 kJ·mol^{-1} than **2a** in the gas phase, which is in line with the experimental observations in the ^{31}P NMR spectra, where **2a^1** was the major mono-borane species in the reaction of **1a/1a^1** with one equivalent of BH_3·THF (Figure 1). The two isomers with nitrogen-bound BH_3 groups (**2a^2** and **2a^3**) exhibit high Gibbs energies $\Delta G°$(298 K) in comparison to **2a** and **2a^1**. Their relative instability is supported by our experiments, where neither the formation of **2a^2** nor **2a^3** could be observed.

Table 2. Relative stability $\Delta G°$(298 K) of different isomers of **2** in kJ·mol^{-1}, evaluated by DFT (B97D, def2-TZVPP).

	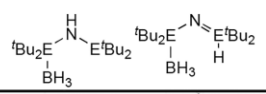	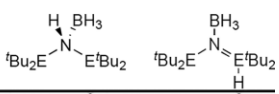
E = P	15.1 (**2a**)	0.0 (**2a^1**)
E = As	0.0 (**2b**)	112.0 (**2b^1**)

E = P	151.4 (**2a^2**)	102.1 (**2a^3**)
E = As	46.4 (**2b^2**)	124.5 (**2b^3**)

Table 3. Relative stability $\Delta G°$(298 K) of different isomers of **3** in kJ·mol^{-1}, evaluated by DFT (B97D, def2-TZVPP).

	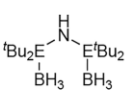	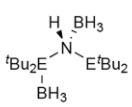	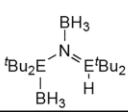
E = P	0.0 (**3a**)	121.0 (**3a^1**)	63.0 (**3a^2**)
E = As	0.0 (**3b**)	130.5 (**3b^1**)	106.7 (**3b^2**)

For the corresponding arsenic compound (E = As), the situation changes. **2b** was found to be the most stable isomer, while **2b^1** is with $\Delta G°$(298 K) = 112.0 kJ·mol^{-1} too high in energy to be observable. The corresponding isomer with a BH_3 group and a proton bound to the central nitrogen atom (**2b^2**) is only 46.6 kJ·mol^{-1} higher in Gibbs energy, whereas **2b^3** is the least stable isomer [$\Delta G°$(298 K) = 124.5 kJ·mol^{-1}] calculated in this series. These findings clearly indicate that the tautomerism observed for phosphorus compounds in this manuscript does not transfer to the corresponding arsenic compounds.

For the *bis*-borane adducts **3**, different isomers were considered as well (Table 3). In agreement with the molecular structures of **3a** and **3b** in the solid state, these were calculated to be the most stable isomers. The isomers with a nitrogen-bound BH_3 group **3a^1** and **3a^2** are found to be 63.0–121.0 kJ·mol^{-1} higher in energy than **3a**. The corresponding isomers of **3b** are 130.5 kJ·mol^{-1} (**3b^1**) and 106.1 kJ·mol^{-1} (**3b^2**) higher in Gibbs energy, which clearly shows that isomers other than those crystallographically characterized are unlikely to be formed in these reactions.

Next, we evaluated whether the formation of certain borane adducts is thermodynamically favorable. In this context, we considered the thermodynamically most stable isomer (see Table 2 and Table 3) for each compound in the calculations. The formation of the mono-borane adducts according to

Equation (1) (see below) is favorable with a $\Delta_R G°(298\ K)$ of –110.7 kJ·mol^{-1} for the formation of **2a^1** and –47.1 kJ·mol^{-1} for **2b**, which confirms the formation of borane adducts is less favorable for the arsenic compound. The formation of the *bis*-borane adducts **3** from the mono adducts **2** according to Equation (2) is in principle less favorable than the formation of mono adducts **2** from **1** and BH_3·THF. Again for the formation of the corresponding arsenic compound **3b** $\Delta_R G°(298\ K)$ is with –25.7 kJ·mol^{-1} lower than for the phosphorus compound **3a** [$\Delta_R G°(298\ K)$ = –47.1 kJ·mol^{-1}], which supports the hypothesis that BH_3-binding in arsenic compounds is weaker than in the corresponding phosphorus compounds:

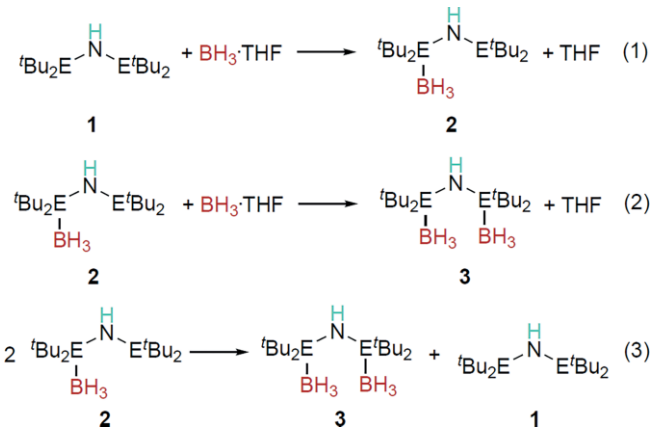

Moreover, we investigated whether the mono adducts **2** are sufficiently stable towards BH_3-transfer according to Equation (3). It becomes evident that the formation of **3a** and **1a** from two equivalents of **2a^1** is thermodynamically uphill by 67.5 kJ·mol^{-1}. The corresponding reaction of the arsenic compound **2b** is only slightly thermodynamically uphill by 21.4 kJ·mol^{-1}.

As the isolation of the mono adducts **2a** or **2a^1** was not possible, we investigated the metalation of mixtures obtained by addition of one equivalent of BH_3·THF to **1a/1a^1** using alkyllithium reagents. Starting from a mixture containing approx. 70 % of the mono adduct **2a** + **2a^1** in addition to **3a** and **1a/1a^1** in toluene, one equivalent *n*BuLi (relative to the initial amount of **1a/1a^1**) was added. Interestingly, only one major reaction product (**4a**) giving rise to a doublet resonance at δ = 89.8 ppm ($^2J_{PP}$ = 64.5 Hz) and quartet of doublets resonance at δ = 61.5 ppm ($^1J_{PB}$ = 112.6, $^2J_{PP}$ = 64.5 Hz) is observed in the $^{31}P\{^1H\}$ NMR spectrum of the reaction mixture. In agreement with the well-resolved resonance for the boron-bound phosphorus atom in the $^{31}P\{^1H\}$ NMR spectrum, we observed a doublet of doublet resonance at –38.8 ppm in the $^{11}B\{^1H\}$ NMR spectrum (Figure 4). The $^7Li\{^1H\}$ NMR spectrum of **4a** displays a single resonance at δ = 0.31 ppm. Overall, the NMR spectroscopic data indicates the formation of a deprotonated phosphine-borane in toluene solution with only one kind of spectroscopically equivalent BH_3 group and lithium ions in an environment with likely coordination of nitrogen atoms. In our efforts to isolate this compound, removal of the solvent in vacuo always led to decomposition. However, we were able to grow some crystals of **4a** directly from the reaction mixture.

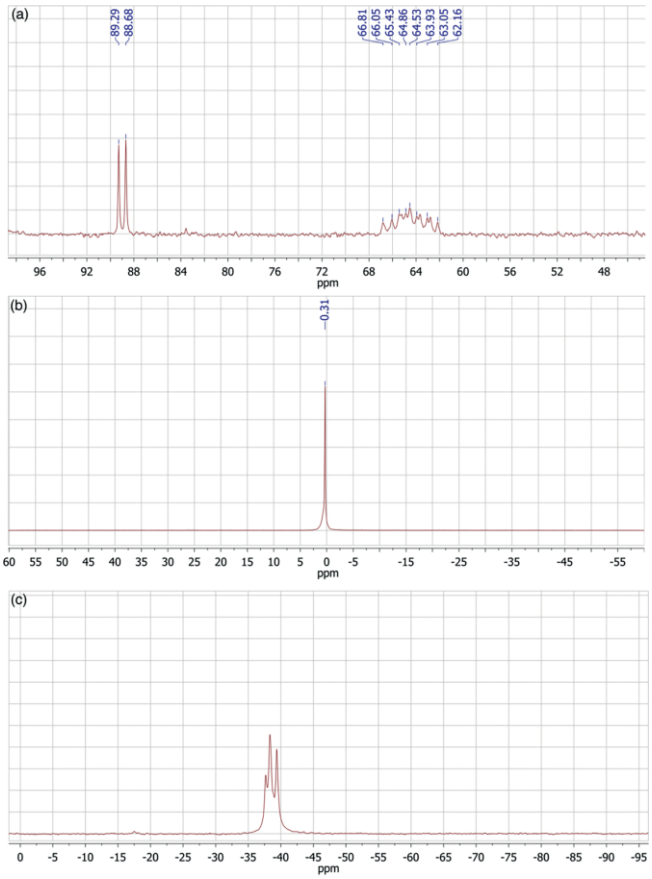

Figure 4. (a) $^{31}P\{^1H\}$ NMR spectrum, (b) $^7Li\{^1H\}$ NMR spectrum, and (c) $^{11}B\{^1H\}$ NMR spectrum of compound **4a**.

An analysis of suitable single crystals of **4a** by single crystal X-ray diffraction revealed the formation of a coordination polymer (Figure 5). The asymmetric unit in the crystal lattice of **4a** contains two different kinds of lithium atoms. Li1 is surrounded by the nitrogen atom of the amide group [*d*(Li1–N2) = 1.920(11) Å] and a η^3-coordinated phosphine-borane group [*d*(Li1–B1) = 2.15(1) Å, *d*(Li1–H) = 1.90(5)–2.27(5) Å], resulting in an overall tetrahedral environment. The second lithium atom Li2 is located in a distorted tetrahedral environment as well, bridging two phosphorus atoms of the phosphine groups [*d*(Li2–P) = 2.562(9)–2.587(9) Å] and a η^2-coordinated phosphine-borane group [*d*(Li2–B2) = 2.32(1) Å]. These coordination patterns finally lead to a situation in which one of the two nitrogen atoms in the asymmetric unit is not bound to lithium. Considering the high ionic contribution in bonds between ligands and lithium, these finding suggest that the charge of the deprotonated phosphine-borane in **4a** is localized on both the nitrogen and the phosphorus atom. In consequence, the groups involving P2 and P4 may alternatively be described as metalated iminophosphorane. Related compounds have been prepared with deprotonated borane adducts of bis(diphenylphosphanyl)-methane,[44,45] but usually the coordination of solvent molecules to the utilized alkaline metal is observed. More importantly, an intramolecular BH_3 group transfer from one phosphorus atom to the deprotonated carbon atom was observed.

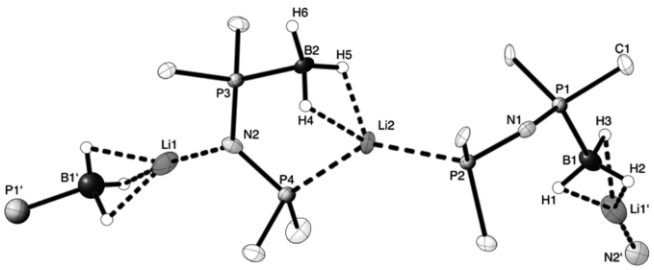

Figure 5. Molecular structure of **4a** in the solid state (*tert*-butyl groups are omitted for clarity, thermal ellipsoids are set at 50 % probability).

In comparison to these examples, the binding motif in **4a** is rather unusual. Moreover, the corresponding lithium complex of the phenyl-substituted *bis*-borane adduct $[Ph_2P(BH_3)\text{-}N\text{-}P(BH_3)Ph_2]^-$ exhibits a central lithium atom in a distorted tetrahedral coordination environment by two THF-ligands and the κ^2-coordinated *bis*-borane.[46] In this compound, the Li–N distances are longer (2.08 Å) than in **4a** and the phosphine-borane group binds in a η^1-fashion. However, the observed bond lengths in **4a** are very similar to related *tert*-butyl-substituted chain compound $t\text{Bu}_2P(BH_3)\text{-NH-BH-NH-P}(BH_3)t\text{Bu}_2$, which was selectively obtained by the reaction of $t\text{Bu}_2\text{P–NH}_2$ with $BH_3{\cdot}SMe_2$.[47]

The fact that the addition of one equivalent of *n*BuLi to a mixture of borane adducts and tautomers leads to a single main product, according to the $^{31}P\{^1H\}$ NMR spectrum of the reaction mixture, suggests the presence of equilibria between the tautomers as well as between **1a** and the other borane adducts, as illustrated in Scheme 1.

Conclusions

In conclusion, we reported a rare example of a tertiary arsine borane adduct (**3b**), of which the structure is compared to the analogous phosphorus compound **3a**. For the mono-borane adducts, it is further demonstrated that in case of the phosphorus compound **2a** two stable isomers can be observed, whereas for the arsenic compound **2b** only one stable isomer was found. The unique coordination polymer **4a** is selectively formed upon addition of base (*n*BuLi) to mixtures of **1a**, **2a**, **3a** and their tautomers. Overall, we reported a very simple approach to prepare chain compounds containing only non-carbon atoms connecting the chain. Based on these results, we will direct our efforts in future investigations towards the preparation of novel main group element based oligomers by the use of different boranes.

Experimental Section

Materials and Methods: All experiments were carried out in an atmosphere of purified argon or nitrogen in the MBraun glove boxes LABmaster 130 and UNIlab or using standard Schlenk techniques. Toluene was distilled from sodium and subsequently stored over 4 Å molecular sieves under argon atmosphere. Deuterated solvents were degassed with freeze-pump-thaw cycles and stored over appropriate molecular sieves under argon atmosphere. $BH_3{\cdot}$THF (1 M in THF) and *n*BuLi (2.5 M in *n*-hexane) were purchased from Aldrich and used as received. Bis(di-*tert*-butylphosphanyl)amine (**1a**) was synthesized following the procedure published by *Chivers* and co-workers.[9] Bis(di-*tert*-butylarsino)amine (**1b**) was synthesized following the procedure published by *Janssen* and *Scherer*.[10]

^1H, ^7Li, ^{13}C, ^{11}B and ^{31}P NMR spectra were recorded using Bruker Avance HD 250, 300 A, DRX 400, DRX 500 and Avance 500 NMR spectrometers at 300 K. ^1H and $^{13}C\{^1H\}$, ^{13}C-APT (attached proton test) NMR chemical shifts are reported in ppm downfield from tetramethylsilane. The resonance of the residual protons in the deuterated solvent was used as internal standard for ^1H NMR spectra. The solvent peak of the deuterated solvent was used as internal standard for ^{13}C NMR spectra. ^{11}B NMR chemical shifts are reported in ppm downfield from $BF_3{\cdot}Et_2O$ and referenced to an external solution of $BF_3{\cdot}Et_2O$ in $CDCl_3$. ^{31}P NMR chemical shifts are reported in ppm downfield from H_3PO_4 and referenced to an external 85 % solution of phosphoric acid in D_2O. The following abbreviations are used for the description of NMR spectroscopic data: br (broad), s (singlet), d (doublet), t (triplet), q (quartet), m (multiplet). FT-IR spectra were recorded by attenuated total reflection of the solid samples on a Bruker Tensor IF37 spectrometer. The intensity of the absorption band is indicated as w (weak), m (medium), s (strong), vs (very strong) and br (broad). HR-ESI mass spectra were acquired with a LTQ-FT mass spectrometer (Thermo Fisher Scientific). The resolution was set to 100.000. Elemental analyses were done by combustion analysis in a vario EL by elementar. In a glovebox, samples were weighed in Sn crucibles and kept under exclusion of ambient air by cold pressure welding. Measurements were performed as double determinations; the values presented herein are the arithmetic mean.

DFT calculations were performed with Grimme's B97D functional including dispersion[48] and the def2-TZVPP basis set after a preoptimization with the def2-SVP basis set[49,50] in Gaussian16.[51] Crystal structures were used as starting models, where possible. After optimization, a frequency calculation was run to ascertain that a ground state was found (no imaginary modes).

Synthesis of 3a: $t\text{Bu}_2\text{P-N(H)-P}t\text{Bu}_2$ (**1a**, 36 mg, 118 µmol) was dissolved in 3 mL toluene and $BH_3{\cdot}$THF (1 M in THF, 240 µL, 240 µmol) was added dropwise to the resulting colorless solution. The progress of the reaction was controlled after 10 min by $^{31}P\{^1H\}$ NMR spectroscopy, which confirmed the selective formation of **3a**. All volatiles were removed in vacuo and the white, partially crystalline residue was dried under vacuum to give 40 mg of **3a** (118 µmol, quant.). Suitable single crystals for the analysis by single crystal X-ray diffraction were obtained by recrystallization from toluene. **^{1}H NMR** (300.1 MHz, C_6D_6, 27 °C): δ = 1.90 (t, br, $^2J_{HP}$ = 5.8 Hz, 1 H, NH), 1.18 (d, $^3J_{HP}$ = 13.0 Hz, 36 H, CH_3), ppm. **^{31}P{^{1}H} NMR** (121.5 MHz, C_6D_6, 27 °C) = 99.5 (q, $^1J_{PB}$ = 51.6 Hz, 2P, P-N-P) ppm. **^{11}B{^{1}H} NMR** (160.5 MHz, C_6D_6, 27 °C): δ = –37.9 (d, $^1J_{BP}$ = 78.1 Hz) ppm. Only resonances whose multiplicity is changing upon ^{31}P and ^{11}B-decoupling are reported in the following $^1H\{^{31}P\}$ NMR and $^1H\{^{11}B\}$ NMR spectra. **^{1}H{^{31}P} NMR** (500.2 MHz, C_6D_6, 27 °C): δ = 1.90 (br. s, 1 H, N*H*), 1.18 (s, 36 H, C*H*$_3$), ppm. **^{1}H{^{11}B} NMR** (500.2 MHz, C_6D_6, 27 °C): δ = 1.47 (dd, $^2J_{HP}$ = 12.8, $^4J_{HH}$ = 3.7 Hz, 6 H, B*H*$_3$) ppm. **^{13}C-APT NMR** (75.5 MHz, C_6D_6, 27 °C): δ = 28.3 [d, $^2J_{CP}$ = 2.0 Hz, *C*$(CH_3)_3$], 19.5 (s, *C*H$_3$) ppm. **IR** (ATR): $\tilde{\nu}$ = 2988 (w), 2963 (m), 2947 (m), 2903 (m), 2870 (m), 2442 (m, νBH), 2384 (m, νBH), 2347 (m, νBH), 2387 (w), 2272 (w), 1472 (m), 1394 (m), 1367 (m), 1310 (s), 1260 (m), 1183 (m), 1143 (m), 1072 (s), 1021 (m), 956 (m), 939 (m), 902 (s), 812 (s), 758 (m), 727 (m), 703 (m), 632 (m), 607 (m), 544 (m), 470 (m), 447 (m) cm^{-1}. **HR-MS** (ESI$^+$) *m*/*z* = 306.2472 (measured), 306.2479 (calculated for $C_{16}H_{38}NP_2$, Δ = 2.3 ppm).

$C_{16}H_{43}B_2NP_2$: found [calcd.] 57.77 [57.66] C, 13.20 [13.34] H, 4.39 % [4.44 %] N.

Synthesis of 3b: *t*Bu_2As-N(H)-As*t*Bu_2 (**1b**, 54 mg, 137 µmol) was dissolved in 4 mL toluene and BH_3·THF (1 M in THF, 2.7 mL, 0.27 mmol) was added dropwise to the resulting colorless solution. After 30 min, all volatiles were removed in vacuo and **3b** was obtained as white and partially crystalline solid (58 mg, 140 µmol, 99 %). Suitable single crystals for the analysis by single crystal X-ray diffraction were obtained by cooling of a saturated toluene solution to 4 °C. **^{1}H NMR** (500.2 MHz, C_6D_6, 27 °C): δ = 1.22 (s, 18 H, CH_3), 1.14 (s, 18 H, CH_3), 1.04 (s br, 1 H, NH) ppm. **^{11}B{^{1}H} NMR** (160.5 MHz, C_6D_6, 27 °C): δ = –37.6 (br. s, 2B, BH_3) ppm. **^{1}H{^{11}B} NMR** (500.2 MHz, C_6D_6, 27 °C): δ = 1.66 (s br, 6 H, As-BH_3) ppm. **^{13}C{^{1}H} NMR** (300.2 MHz, C_6D_6, 27 °C): δ = 40.2 [s, 2C, $C(CH_3)_3$], 37.2 [s, 2C, $C(CH_3)_3$], 28.9 [s, 6C, C(CH_3)$_3$], 27.9 [s, 6C, C(CH_3)$_3$] ppm. **IR** (ATR): $\tilde{\nu}$ = 2961 (w), 2939 (w), 2892 (w), 2862 (w), 2440 (w, νBH), 2406 (w, νBH), 2356 (w, νBH), 2260 (w), 1465 (m), 1417 (m), 1393 (m), 1365 (m), 1337 (m), 1259 (m), 1237 (m), 1169 (m), 1138 (m), 1089 (m), 1052 (s), 1016 (s), 937 (w), 864 (w), 793 (s), 772 (s), 723 (s), 577 (w), 543 (w), 478 (w), 409 (w) cm^{-1}. **HR-MS** (ESI$^+$) *m*/*z* = 410.1383 (measured), 410.1380 (calculated for $C_{16}H_{18}NAs_2O$, Δ = 0.7 ppm); 426.1329 (measured), 426.1330 (calculated for $C_{16}H_{38}NAs_2O_2$, Δ = 0.2 ppm). $C_{16}H_{43}As_2B_2N$: found [calcd.] 45.71 [45.65] C, 9.89 [10.30] H, 2.72 % [3.33 %] N.

Formation of 4a: *t*Bu_2P-N(H)-P*t*Bu_2 (**1a**, 46 mg, 151 µmol) was dissolved in 5 mL toluene or THF and BH_3·THF (0.1 M in THF, 1.5 mL, 0.15 mmol) was added dropwise to the resulting colorless solution. After fifteen min of stirring at ambient temperature, *n*BuLi (2.5 M in *n*-hexane, 0.06 mL, 150 µmol) was added dropwise and the mixture was allowed to stir for further 60 min and analyzed by NMR spectroscopy. Cooling of the solution results in the formation of crystals after a couple weeks, which were suitable for the analysis by single crystal X-ray diffraction. As compound **4a** turns out to be unstable under vacuum, it was not possible to obtain a fitting bulk analysis for **4a**. **^{1}H NMR** (300.1 MHz, C_6D_6, 27 °C): δ = 1.51 [d, $^2J_{HP}$ = 12.0 Hz, 9 H, C(CH_3)$_3$], 1.40 [d, $^2J_{HP}$ = 11.4 Hz, 9 H, C(CH_3)$_3$], 1.34 [d, $^2J_{HP}$ = 12.4 Hz, 9 H, C(CH_3)$_3$], 1.00 [d, $^2J_{HP}$ = 16.0 Hz, 9 H, C(CH_3)$_3$] ppm. **^{31}P{^{1}H} NMR** (121.5 MHz, THF, 27 °C) = 89.8 (d, $^2J_{PP}$ = 64.5 Hz, 1P, P*t*Bu_2), 61.5 (dq, $^1J_{PB}$ = 112.6, $^2J_{PP}$ = 64.5, 1P, PBH_3) ppm. **^{11}B{^{1}H} NMR** (96.3 MHz, C_6D_6, 27 °C): δ = –38.8 (dd, $^1J_{BP}$ = 108.7, $^3J_{BP}$ = 55.7 Hz, 1B, BH_3) ppm. Only resonances whose multiplicity is changing upon ^{11}B-decoupling are reported in the following ^{1}H{^{11}B} NMR spectra. **^{1}H{^{11}B} NMR** (300.3 MHz, C_6D_6, 27 °C): δ = 0.69 (d, $^2J_{HP}$ = 12.7 Hz, 3 H, BH_3) ppm. **^{7}Li{^{1}H} NMR** (116.7 MHz, C_6D_6, 27 °C): δ = 0.31 (br. s, N-Li) ppm. **^{13}C-APT NMR** (75.5 MHz, C_6D_6, 27 °C): δ = 35.9 [d, $^1J_{CP}$ = 11.4 Hz, 2C, $C(CH_3)_3$], 35.8 [d, $^1J_{CP}$ = 11.6 Hz, 2C, $C(CH_3)_3$], 30.2 [d, $^2J_{CP}$ = 12.8 Hz, 6C, C(CH_3)$_3$], 29.5 [d, 6C, C(CH_3)$_3$] ppm. **IR** (ATR): $\tilde{\nu}$ = 2980 (m), 2952 (m), 2927 (m), 2896 (m), 1864 (m), 2387 (m, BH), 2287 (m, BH), 1474(m), 1386 (m), 1359 (m), 1308 (s), 1239 (m), 1203 (m), 1174 (m), 1088 (s), 1045 (s), 1032 (s), 1017 (s), 958 (m), 936 (m), 914 (m), 893 (w), 866 (w), 812 (s), 756 (w), 726 (w), 703 (m), 656 (w), 632 (m), 608 (w), 581 (w), 555 (m), 539 (m), 517 (w), 490 (s), 443 (s) cm^{-1}. **HR-MS** (ESI$^+$) *m*/*z* = 306.2474 (measured), 306.2479 (calculated for $C_{16}H_{38}NP_2$, Δ = 1.6 ppm).

Supporting Information (see footnote on the first page of this article): Detailed crystallographic information, NMR spectra, and details on the DFT calculations.

Acknowledgements

We gratefully acknowledge financial support from the Deutsche Forschungsgemeinschaft (LA 2830/6–1), for funding R. L. within the Heisenberg-program (LA 2830/8–1). Open access funding enabled and organized by Projekt DEAL.

Keywords: Phosphorus; Arsenic; Boron; Group 13/15 compounds; Lewis acid base adducts

References

[1] A. Staubitz, A. P. M. Robertson, M. E. Sloan, I. Manners, *Chem. Rev.* **2010**, *110*, 4023–4078.
[2] P. Pellon, *Tetrahedron Lett.* **1992**, *33*, 4451–4452.
[3] M. J. Brunel, B. Faure, M. Maffei, *Coord. Chem. Rev.* **1998**, *180*, 665–698.
[4] B. Carboni, L. Monnier, *Tetrahedron* **1999**, *55*, 1197–1248.
[5] M. Ohff, J. Holz, M. Quirmbach, A. Börner, *Synthesis* **1998**, 1391–1415.
[6] L. Maser, L. Vondung, R. Langer, *Polyhedron* **2018**, *143*, 28–42.
[7] L. Vondung, N. Frank, M. Fritz, L. Alig, R. Langer, *Angew. Chem. Int. Ed.* **2016**, *55*, 14450–14454.
[8] L. Vondung, L. E. Sattler, R. Langer, *Chem. Eur. J.* **2018**, *24*, 1358–1364.
[9] J. S. Ritch, T. Chivers, D. J. Eisler, H. M. Tuononen, *Chem. Eur. J.* **2007**, *13*, 4643–4653.
[10] O. J. Janssen, W. Scherer, *J. Organomet. Chem.* **1969**, *16*, P69–P70.
[11] G. I. Nikonov, A. J. Blake, D. A. Lemenovskii, S. Wocadlo, *J. Organomet. Chem.* **1997**, *547*, 235–242.
[12] O. Hegen, A. V. Virovets, A. Y. Timoshkin, M. Scheer, *Chem. Eur. J.* **2018**, *24*, 16521–16525.
[13] O. Hegen, J. Braese, A. Y. Timoshkin, M. Scheer, *Chem. Eur. J.* **2019**, *25*, 485–489.
[14] R. A. J. K. Chadha, J. M. Chehayber, J. E. Drake, *J. Cryst. Spec. Res.* **1985**, *15*, 53–60.
[15] J. Burt, J. W. Emsley, W. Levason, G. Reid, I. S. Tinkler, *Inorg. Chem.* **2016**, *55*, 8852–8864.
[16] A. M. Priegert, B. W. Rawe, S. C. Serin, D. P. Gates, *Chem. Soc. Rev.* **2016**, *45*, 922–953.
[17] B. W. Rawe, C. P. Chun, D. P. Gates, *Chem. Sci.* **2014**, *5*, 4928–4938.
[18] O. Ayhan, N. A. Riensch, C. Glasmacher, H. Helten, *Chem. Eur. J.* **2018**, *24*, 5883–5894.
[19] O. Ayhan, T. Eckert, F. A. Plamper, H. Helten, *Angew. Chem. Int. Ed.* **2016**, *55*, 13321–13325.
[20] H. R. Allcock, *Dalton Trans.* **2016**, *45*, 1856–1862.
[21] C. Marquardt, T. Jurca, K. C. Schwan, A. Stauber, A. V. Virovets, G. R. Whittell, I. Manners, M. Scheer, *Angew. Chem. Int. Ed.* **2015**, *54*, 13782–13786.
[22] A. Staubitz, A. P. Soto, I. Manners, *Angew. Chem. Int. Ed.* **2008**, *47*, 6212–6215.
[23] V. Blackstone, A. Presa Soto, I. Manners, *Dalton Trans.* **2008**, 4363.
[24] T. Sanji, in *Main Group Strategies Toward Functional Hybrid Materials* (Eds.: T. Baumgartner, F. Jäkle), Wiley, Chichester, UK, **2018**, pp. 197–208.
[25] A. Mitra, D. A. Atwood, in *Encycl. Inorganic Bioinorganic Chemistry* (Ed.: R. A. Scott), Wiley, Chichester, UK, **2006**.
[26] S. Rothemund, I. Teasdale, *Chem. Soc. Rev.* **2016**, *45*, 5200–5215.
[27] J. Linshoeft, E. J. Baum, A. Hussain, P. J. Gates, C. Näther, A. Staubitz, *Angew. Chem. Int. Ed.* **2014**, *53*, 12916–12920.
[28] Z. M. Hudson, D. J. Lunn, M. A. Winnik, I. Manners, *Nat. Commun.* **2014**, *5*, 3372.
[29] X. He, T. Baumgartner, *RSC Adv.* **2013**, *3*, 11334–11350.

[30] R. Allcock, *Chem. Mater.* **1994**, *6*, 1476–1491.
[31] M. Liang, I. Manners, *J. Am. Chem. Soc.* **1991**, *113*, 4044–4045.
[32] P. J. Fazen, J. S. Beck, A. T. Lynch, E. E. Remsen, L. G. Sneddon, *Chem. Mater.* **1990**, *2*, 96–97.
[33] R. D. Miller, J. Michl, *Chem. Rev.* **1989**, *89*, 1359–1410.
[34] F. Vidal, F. Jäkle, *Angew. Chem. Int. Ed.* **2019**, *58*, 5846–5870.
[35] O. Hegen, C. Marquardt, A. Y. Timoshkin, M. Scheer, *Angew. Chem. Int. Ed.* **2017**, *56*, 12783–12787.
[36] C. Marquardt, A. Adolf, A. Stauber, M. Bodensteiner, A. V. Virovets, A. Y. Timoshkin, M. Scheer, *Chem. Eur. J.* **2013**, *19*, 11887–11891.
[37] C. Marquardt, J. Baumann, A. V. Virovets, M. Scheer, *Chem. Eur. J.* **2017**, *23*, 11423–11429.
[38] C. Marquardt, T. Kahoun, A. Stauber, M. Bodensteiner, A. Y. Timoshkin, M. Scheer, *Angew. Chem. Int. Ed.* **2016**, *55*, 14828–14832.
[39] C. Marquardt, C. Thoms, A. Stauber, G. Balµzs, M. Bodensteiner, M. Scheer, *Angew. Chem. Int. Ed.* **2014**, *53*, 3727–3730.
[40] J. Braese, A. Schinabeck, M. Bodensteiner, H. Yersin, A. Y. Timoshkin, M. Scheer, *Chem. Eur. J.* **2018**, *24*, 10073–10077.
[41] K. Schwan, A. Adolf, C. Thoms, M. Zabel, Y. Timoshkin, M. Scheer, *Dalton Trans.* **2008**, 5054–5058.
[42] U. Vogel, K. Schwan, P. Hoemensch, M. Scheer, *Eur. J. Inorg. Chem.* **2005**, 1453–1458.
[43] H. Nöth, E. Fluck, *Z. Naturforsch. B* **1984**, *39*, 744–753.
[44] J. Langer, K. Wimmer, H. Görls, M. Westerhausen, *Dalton Trans.* **2009**, *22*, 2951–2957.
[45] J. Langer, V. K. Pálfi, H. Görls, M. Reiher, M. Westerhausen, *Chem. Commun.* **2013**, *49*, 1121.
[46] J. Bhattacharjee, S. Das, T. D. N. Reddy, P. Nayek, B. S. Mallik, T. K. Panda, *Z. Anorg. Allg. Chem.* **2016**, *3*, 118–127.
[47] M. Köster, A. Kreher, C. Von Hänisch, *Dalton Trans.* **2018**, *47*, 7875–7878.
[48] S. Grimme, *J. Comput. Chem.* **2006**, *27*, 1787–1799.
[49] F. Weigend, C. Hättig, H. Patzelt, R. Ahlrichs, S. Spencer, A. Willets, *Phys. Chem. Chem. Phys.* **2006**, *8*, 1057.
[50] F. Weigend, R. Ahlrichs, K. A. Peterson, T. H. Dunning, R. M. Pitzer, A. Bergner, *Phys. Chem. Chem. Phys.* **2005**, *7*, 3297.
[51] M. J. Frisch, G. W. Trucks, H. B. Schlegel, G. E. Scuseria, M. A. Robb, J. R. Cheeseman, G. Scalmani, V. Barone, G. A. Petersson, H. Nakatsuji, et al., Gaussian16, Inc., Wallingford CT, **2016**.

Received: January 28, 2020

